Available online at www.sciencedirect.com
SCIENCE DIRECT®
Journal of Crystal Growth 287 (2006) 615–619
JOURNAL OF CRYSTAL GROWTH
www.elsevier.com/locate/jcrysgro

Characteristics of InGaAsN-GaAsSb type-II "W" quantum wells

J.-Y. Yeh[a,*], L.J. Mawst[a], A.A. Khandekar[b], T.F. Kuech[b], I. Vurgaftman[c], J.R. Meyer[c], N. Tansu[d]

[a]*Department of Electrical and Computer Engineering, University of Wisconsin-Madison, 1415 Engineering Drive, Madison, WI 53706, USA*
[b]*Department of Chemical and Biological Engineering, University of Wisconsin, Madison, USA*
[c]*Code 5613, Naval Research Laboratory, Washington, DC 20375, USA*
[d]*Department of Electrical and Computer Engineering, Center for Optical Technologies, Lehigh University, Bethlehem, PA 18015, USA*

Abstract

InGaAsN-GaAsSb type-II "W" quantum well structures have been grown by metalorganic chemical vapor deposition (MOCVD). Photoluminescence and X-ray diffraction measurements indicate that thin layers (2–2.5 nm) of $GaAs_{1-y}Sb_y$ and $InGaAs_{1-x}N_x$ can be grown with compositions of $y = 0.3$ and $x = 0.02$. "W" structures with different N contents indicate that emission wavelengths in the 1.4–1.6 μm range can be achieved. The use of $GaAs_{0.85}P_{0.15}$ tensile strained barrier layers is found to significantly improve the photoluminescence intensity of the "W" structure and result in a wavelength blueshift.

Keywords: A1. Epitaxy; A3. Metalorganic chemical vapor deposition; A3. Type-II quantum well; B3. Near-infrared

1. Introduction

High performance and inexpensive long wavelength (1300–1550 nm) emitting diode lasers on GaAs substrates are essential components for optical fiber communication systems. For 1300-nm emission wavelengths, diode lasers with active regions of highly strained InGaAsN quantum wells (QWs) [1], GaAsSb QWs [2,3], InAs quantum dots [4] and InGaAs-GaAsSb type-II QWs [5] have been demonstrated. However, in the 1550-nm regime, these methods encounter great difficulties in terms of wavelength limitation and device performance degradation [6,7]. To overcome this problem, a dilute-nitride type-II InGaAs-GaAsSb QW structure was proposed [8,9] for achieving 1550-nm on GaAs, as shown in the schematic band diagram in Fig. 1. In this structure, InGaAsN is used as the electron well and GaAsSb as the hole well, allowing the emission wavelength to be engineered over a large range. The optimal design of the type-II QW for maximizing the optical gain is to utilize the "W" shape configuration, i.e. a GaAsSb hole well sandwiched by two InGaAsN electron wells. In addition, this design exhibits good carrier confinement for both electrons (~330 meV) and holes (~200–300 meV) according to our simulation study, thus low device temperature sensitivity is expected. Due to the nature of the type-II optical transition, the material gain of the "W" structure depends strongly on the spatial overlap between electron and hole wave functions. Using a 10-band $k \cdot p$ formalism, it has been shown that by utilizing very thin InGaAsN and GaAsSb layers (around 2–3 nm), wave function overlaps of 50% similar to GaSb-based type-II QWs can be achieved [10]. Therefore, experimentally, the ability to obtain high material quality with low defect density and abrupt interfaces for the thin QW layers is extremely important. In this work, we focus on the metalorganic chemical vapor deposition (MOCVD) growth and characterization of the type-II QW active region.

2. Material epitaxy of the InGaAsN–GaAsSb type-II QW

2.1. GaAsSb epitaxy

GaAsSb layers were grown at a temperature of 530 °C and reactor pressure of 100 mbar. The material precursors

*Corresponding author. Tel. +1 608 265 5403; fax: +1 608 265 4623.
E-mail address: jyeh@cae.wisc.edu (J.-Y. Yeh).

0022-0248/$ - see front matter © 2005 Published by Elsevier B.V.
doi:10.1016/j.jcrysgro.2005.10.087

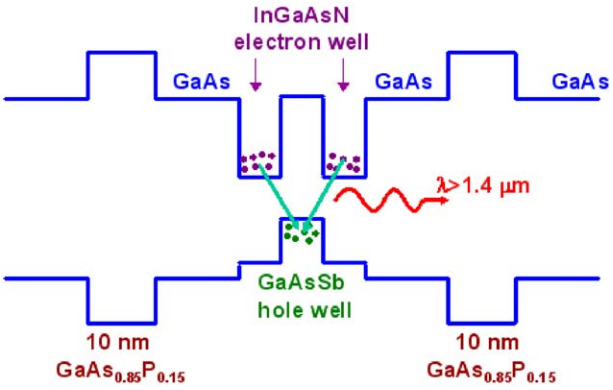

Fig. 1. The schematic band diagram of the InGaAsN–GaAsSb type-II "W" QW structure. The tensile-strained GaAsP barriers can effectively compensate the high compressive strain of the active region.

for GaAsSb were trimethylgallium (TMGa), arsine (AsH_3) and trimethylantimony (TMSb). The key for growing high quality GaAsSb is to utilize a low V/III ratio, typically around 1 [11]. To calibrate the material growth condition, a series of GaAsSb–GaAs superlattice (SL) samples with various V/III ratios have been grown. Fig. 2(a) shows the results of high-resolution X-ray diffraction (HRXRD) measurement, while Fig. 2(b) shows transmission electron microscope (TEM) images of the GaAsSb–GaAs SL structure. The GaAsSb layer and GaAs barrier thicknesses are 2 and 18 nm, respectively. The growth rate of GaAsSb and GaAs were calibrated to be 90 and 186 Å/min, respectively. With the thickness information from the TEM image, the material solid composition can be determined by fitting the experimental X-ray diffraction pattern with the dynamic simulation data. The layer thicknesses served as the known parameters in the X-ray data simulation. For the GaAsSb layer, the V/III ratio was 1.34 and gas phase Sb/V ratio was 85%, resulting in a solid phase antimony content near 30%. The high Sb-content is required to achieve a large valence band offset and therefore long wavelength emission. To improve the interface between GaAsSb and GaAs, special care must be taken during the gas switching [12]. At the GaAs-to-GaAsSb interface, AsH_3 and TMSb was applied for a duration of 5 s in order to establish the presence of the antimony precursor, followed by the introduction of TMGa, i.e., the onset of GaAsSb layer growth. The TMSb pre-purge procedure is used to improve Sb incorporation into the grown material. At the GaAsSb-to-GaAs interface, all group V supplies were immediately terminated after the GaAsSb layer growth, while maintaining the TMGa flow for 1 s. Following the 1 s TMGa flow, a low AsH_3 flow was introduced. The purpose of the 1-s TMGa purge is to utilize the group-III metal to collect the floating Sb atoms on top of the epitaxial surface [12]. It is well known that at the GaAsSb to GaAs interface, severe antimony segregation during the growth process results in a graded interface [13]. Employing this gas-switching

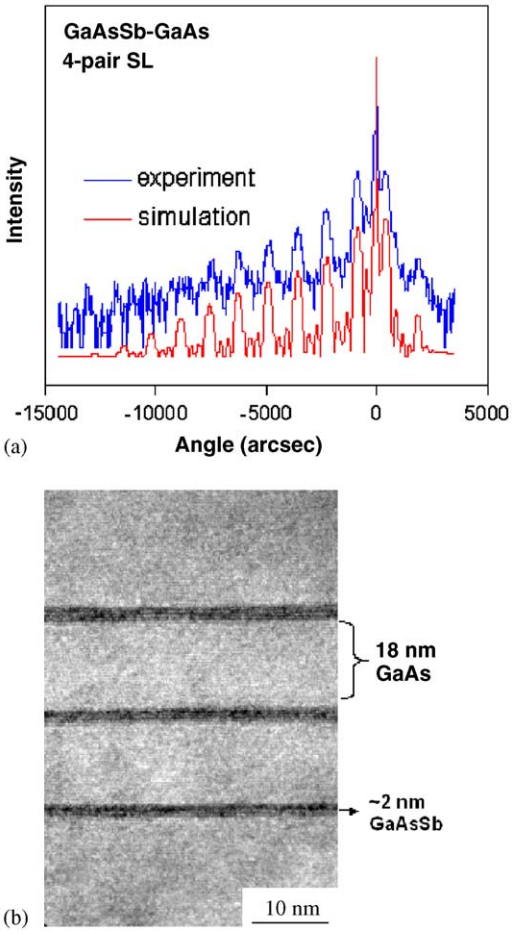

Fig. 2. (a) The (0 0 4) ω–2θ X-ray diffraction pattern of a 4-pair GaAsSb–GaAs superlattice. (b) The TEM image of the GaAsSb–GaAs structure. The GaAsSb layer thickness of 2 nm and Sb-content of 30% are calibrated.

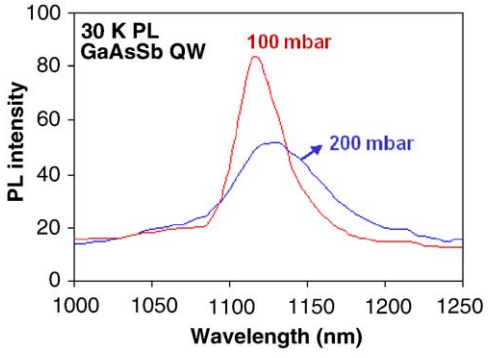

Fig. 3. Comparison of 30 K PL spectrum of the GaAsSb–GaAs QW structure grown with MOCVD reactor pressure of 100 and 200 mbar.

scheme, both the HRXRD fringe pattern and TEM image in Fig. 2 reveal the sharp and well-defined interfaces between GaAsSb and GaAs.

Fig. 3 shows the low temperature PL spectrum of the GaAsSb–GaAs SL structures (2-nm/18-nm) grown at reactor pressures of 100 and 200 mbar. The V/III ratio

was 1.34 for both samples. We find that a lower reactor pressure significantly improves the PL intensity (2×) as well as the spectral full width half maximum (FWHM). It is believed that a lower reactor pressure enhances gas transport and switching speed and therefore results in sharper interfaces, and the effect is especially perceptible for case of the GaAsSb-GaAs SL structure.

2.2. InGaAsN epitaxy

The InGaAsN layers were grown at the temperature of 530 °C and reactor pressure of 100 mbar, identical to those of the GaAsSb epitaxy. The material precursors for InGaAsN were TMGa, trimethylindium (TMIn), AsH_3, and dimethylhydrazine (DMHy). The growth rate and composition were also calibrated by the HRXRD experiments on the SL samples as shown in Fig. 4. Three samples of the InGaAsN–GaAs SL with various nitrogen contents were grown and characterized. For the sake of simplicity, the TMGa, TMIn and DMHy flows were kept constant for all three samples and the solid phase nitrogen content was controlled by adjusting AsH_3 gas flow. The indium content was 37% and the InGaAsN (GaAs barrier) thickness was 2.5 nm (17.5 nm). The growth rate for InGaAsN was 285 Å/min. The gas phase DMHy to group V (N/V) ratios were equal to 0.994, 0.995 and 0.996. The resulting solid phase nitrogen contents were in the range of 2% for $N/V = 0.994$ and 2.2% for $N/V = 0.995$. For comparison purposes, a nitrogen-free InGaAs–GaAs SL structure was also characterized, as shown in Fig. 4.

According to the HRXRD data, it appears that the epitaxial layer remains high quality as the N/V ratio increases (i.e., high signal-to-noise ratio of the fringe pattern), but suddenly shows degradation for a N/V ratio equal to 0.996. The deterioration of the X-ray diffraction pattern of this SL structure may indicate the onset of a 3D growth mode for the InGaAsN layers, resulting in rough interfaces. The nitrogen content of this sample ($N/V = 0.996$) was difficult to determine due to its poor fringe pattern.

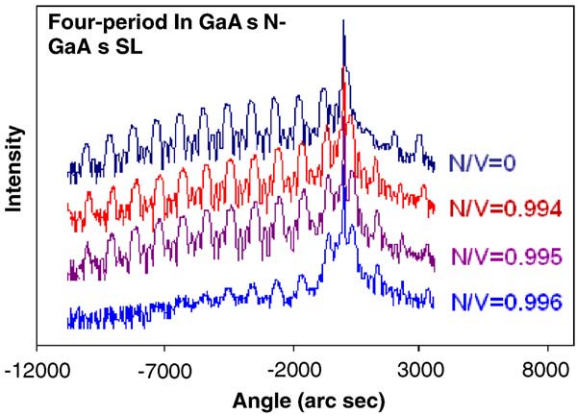

Fig. 4. The (0 0 4) $\omega-2\theta$ X-ray diffraction pattern of a 4-pair InGaAsN–GaAs superlattice. By adjusting the N/V values, various nitrogen contents in InGaAsN layers can be achieved.

3. InGaAsN–GaAsSb type-II QW epitaxy and PL characterization

The schematic band structure of the InGaAsN–GaAsSb type-II QW is shown in Fig. 1. Utilizing the MOCVD epitaxy studies of GaAsSb and InGaAsN discussed above, the antimony content in this structure was fixed at 30% and the nitrogen content served as a variable for emission wavelength engineering. The layer thickness of the GaAsSb and InGaAsN was 2 nm and 2.5 nm, respectively. As shown in Fig. 1, tensile strained $GaAs_{0.85}P_{0.15}$ layers were employed in this structure for strain compensation purposes due to the compressively strained GaAsSb and InGaAsN layers ($\Delta a/a > 2\%$). The gas switching scheme at the GaAsSb and InGaAsN interfaces was the same as for the GaAsSb/GaAs SL discussed in Section 2.1. Room temperature and low temperature PL experiments were conducted to examine the optical quality of the type-II QW structure. To study the impact of thermal annealing on PL intensity and emission wavelength, samples were in-situ annealed at 640 °C in AsH_3/H_2 and cooled down in N_2 ambient.

Fig. 5 shows the low temperature (30 K) PL spectrum of three InGaAsN–GaAsSb type-II "W" QW structures with N/V ratios ranging from 0.994 to 0.996. These samples were subject to only 3 min of high temperature thermal annealing treatment during growth of the top AlGaAs cladding layer. The Argon laser excitation power density was 20 W/cm^2 for this measurement. The emission wavelengths are 1425, 1480 and 1620 nm for the samples with $N/V = 0.994$, 0.995 and 0.996, respectively. Without nitrogen, the InGaAs–GaAsSb type-II QW exhibits 30 K peak wavelength at 1260 nm. The PL spectrum FWHM

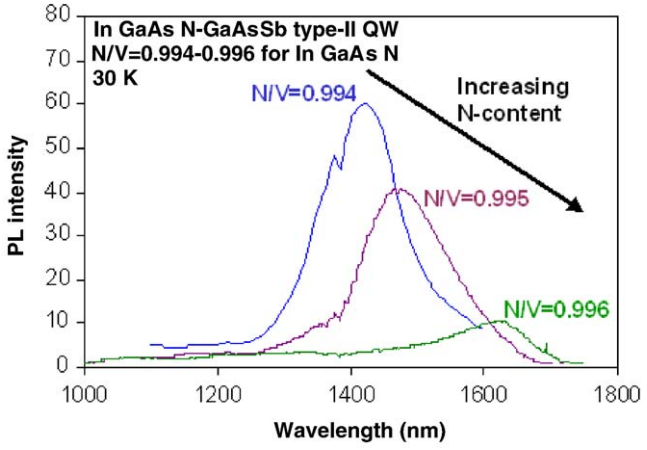

Fig. 5. 30 K PL spectrum of the InGaAsN–GaAsSb type-II "W" QW structures grown with gas phase N/V ratios from 0.994 to 0.996. Significant wavelength red shift was observed with increasing nitrogen-content in the InGaAsN layers.

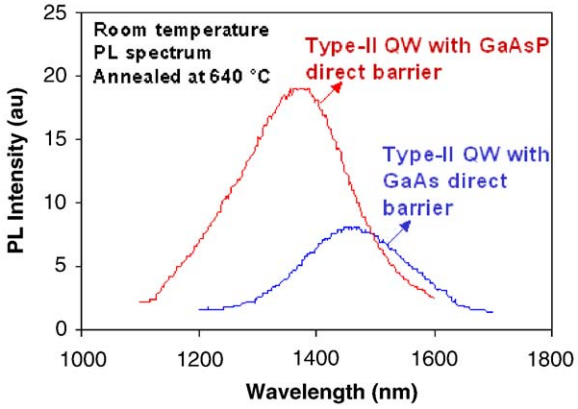

Fig. 6. Room temperature (300 K) PL spectrum of the type-II "W" QW with GaAsP or GaAs direct barrier. Both samples were annealed at 640 °C for 25 min under AsH_3 and H_2 ambient.

increases from 30 meV for the nitrogen-free sample to 78–88 meV for the samples with high nitrogen content, indicating the possibility of some degree of phase separation in the InGaAsN. Significant degradations of the PL intensity and FWHM for the 1620-nm emitting sample are presumably due to the onset of three-dimensional growth mode under such an extremely high N/V ratio, which was suggested by the HRXRD experiments shown in Fig. 4.

One method to improve the carrier confinement and PL intensity is to utilize a larger bandgap material as the barrier directly surrounding the InGaAsN QW. With GaAsP as the barrier, 1300-nm InGaAsN QW lasers were reported with low threshold current, high efficiency, and most importantly, the temperature performance of the devices was superior to the standard InGaAsN QW lasers with GaAs direct barriers [14]. Fig. 6 shows the room temperature PL spectrum of two InGaAsN–GaAsSb type-II "W" QW structures with either GaAsP or GaAs direct barriers. The InGaAsN layers were grown with the condition of $N/V = 0.995$. These two samples were both subject to 640 °C thermal annealing for 25 min to reduce the nonradiative defect centers formed during the epitaxial process and improve the optical quality [15]. The QW with the GaAsP direct barriers exhibit a higher PL intensity ($2\times$) and a significant wavelength blue shift, from 1462 nm for the GaAs direct barrier sample to 1374 nm. Two mechanisms can lead to such a blue shift, which was also observed previously in type-I InGaAsN QWs with GaAsP direct barriers [14]. First, because of the higher potential barrier, the quantum confinement effect contributes to a larger transition energy. Secondly, with a GaAsP barrier right up against the QW, the possibility of phosphorous incorporation in the well may reduce the nitrogen incorporation efficiency. This spectral blue shift behavior was also reported by Koyama and coworkers, although the finding that the InGaAsN(P) QW actually had a lower PL intensity which contradicts to our finding for the type-II QW [16].

4. Summary

In summary, to realize GaAs-based 1550-nm emitting diode lasers, long wavelength emission from the InGaAsN–GaAsSb type-II "W" QW structures has been demonstrated by MOCVD growth technique. Growth conditions and the interface gas switching sequence have been investigated in detail. Low temperature PL experiments show that the emission wavelength from this structure can reach the 1400–1600 nm range. MOCVD epitaxy optimization to achieve high material quality of the very thin layers in the type-II QW structure is essential and more studies need to be done. Nevertheless, the room temperature PL result shows that the type-II "W" QW design is a promising candidate for realizing long wavelength GaAs-based diode lasers beyond 1500 nm.

Acknowledgments

This work was supported by the Army Research Office and NSF Grant no. 0355442.

Reference

[1] N. Tansu, N.J. Kirsch, L.J. Mawst, Low-threshold-current-density 1300-nm dilute-nitride quantum well lasers, Appl. Phys. Lett. 81 (14) (2002) 2523.
[2] R. Dowd, S.R. Johnson, S.A. Feld, M. Adamcyk, S.A. Chaparro, J. Joseph, K. Hilgers, M.P. Horning, K. Shiralagi, Y.H. Zhang, Long wavelength GaAsP/GaAs/GaAsSb VCSELs on GaAs substrates for communications applications, Electron. Lett. 39 (13) (2003) 987.
[3] S.W. Ryu, P.D. Dapkus, Low threshold current density GaAsSb quantum well (QW) lasers grown by metal organic chemical vapour deposition on GaAs substrates, Electron. Lett. 36 (16) (2000) 1387.
[4] E.C. Le Ru, P. Howe, T.S. Jones, R. Murray, Strain-engineered InAs/GaAs quantum dots for long-wavelength emission, Phys. Rev. B 67 (16) (2003).
[5] S.W. Ryu, P.D. Dapkus, Room temperature operation of type-II GaAsSb/InGaAs quantum well laser on GaAs substrates, Electron. Lett. 38 (12) (2002) 564.
[6] M. Yokozeki, J. Mitomo, Y. Sato, T. Hino, H. Narui, 1.50 mu m CW operation of GalnNAs/GaAs laser diodes grown by MOCVD, Electron. Lett. 40 (17) (2004) 1060.
[7] J.Y. Yeh, L.J. Mawst, N. Tansu, Characteristics of InGaAsN/GaAsN quantum well lasers emitting in the 1.4-μm regime, J. Crystal Growth 272 (1–4) (2004) 719.
[8] N. Tansu, L.J. Mawst, Design analysis of 1550-nm GaAsSb–(In)-GaAsN type-II quantum-well laser active regions, IEEE J. Quant. Electron. 39 (10) (2003) 1205.
[9] I. Vurgaftman, J.R. Meyer, N. Tansu, L.J. Mawst, (In)GaAsN-based type-II "W" quantum-well lasers for emission at lambda = 1.55 μm, Appl. Phys. Lett. 83 (14) (2003) 2742.
[10] J.R. Meyer, C.A. Hoffman, F.J. Bartoli, L.R. Rammohan, Type-Ii Quantum-Well Lasers for the Midwavelength Infrared, Appl. Phys. Lett. 67 (6) (1995) 757.
[11] J. Shin, T.C. Hsu, Y. Hsu, G.B. Stringfellow, OMVPE growth of metastable GaAsSb and GaInAsSb alloys using TBAs and TBDMSb, J. Crystal Growth 179 (1–2) (1997) 1.
[12] B.E. Hawkins, A.A. Khandekar, J.Y. Yeh, L.J. Mawst, T.F. Kuech, Effects of gas switching sequences on GaAs/GaAs1-Sb-y(y) superlattices, J. Crystal Growth 272 (1–4) (2004) 686.

[13] R. Kaspi, K.R. Evans, Sb-surface segregation and the control of compositional abruptness at the GaAsSb/GaAs interface, J. Crystal Growth 175 (1997) 838.

[14] N. Tansu, J.Y. Yeh, L.J. Mawst, Physics and characteristics of high performance 1200 nm InGaAs and 1300–1400 nm InGaAsN quantum well lasers obtained by metal-organic chemical vapour deposition, J. Phys. Condensed Matter 16 (31) (2004) S3277.

[15] T. Kitatani, K. Nakahara, M. Kondow, K. Uomi, T. Tanaka, Mechanism analysis of improved GaInNAs optical properties through thermal annealing, J. Crystal Growth 209 (2–3) (2000) 345.

[16] M. Kawaguchi, T. Miyamoto, A. Saitoh, F. Koyama, Photoluminescence and lasing characteristics of GaInNAs/GaAsP strain-compensated quantum wells, Jpn J. Appl. Phys. Lett. 43 (2B) (2004) L267.